



Original Article

# Mesenchymal Stem Cells Alleviate Acute Liver Failure through Regulating Hepatocyte Apoptosis and Macrophage Polarization



Yachao Tao<sup>1,2</sup>, Yonghong Wang<sup>1,2</sup>, Menglan Wang<sup>1,2</sup>, Hong Tang<sup>1,2\*</sup> and Enqiang Chen<sup>1,2\*</sup> 

<sup>1</sup>Center of Infectious Diseases, West China Hospital, Sichuan University, Chengdu, Sichuan, China; <sup>2</sup>Division of Infectious Diseases, State Key Laboratory of Biotherapy, Sichuan University, Chengdu, Sichuan, China

Received: January 09, 2024 | Revised: March 06, 2024 | Accepted: March 18, 2024 | Published online: April 30, 2024

## Abstract

**Background and Aims:** Acute liver failure (ALF) is a life-threatening clinical problem with limited treatment options. Administration of human umbilical cord mesenchymal stem cells (hUC-MSCs) may be a promising approach for ALF. This study aimed to explore the role of hUC-MSCs in the treatment of ALF and the underlying mechanisms. **Methods:** A mouse model of ALF was induced by lipopolysaccharide and d-galactosamine administration. The therapeutic effects of hUC-MSCs were evaluated by assessing serum enzyme activity, histological appearance, and cell apoptosis in liver tissues. The apoptosis rate was analyzed in AML12 cells. The levels of inflammatory cytokines and the phenotype of RAW264.7 cells co-cultured with hUC-MSCs were detected. The C-Jun N-terminal kinase/nuclear factor-kappa B signaling pathway was studied. **Results:** The hUC-MSCs treatment decreased the levels of serum alanine aminotransferase and aspartate aminotransferase, reduced pathological damage, alleviated hepatocyte apoptosis, and reduced mortality *in vivo*. The hUC-MSCs co-culture reduced the apoptosis rate of AML12 cells *in vitro*. Moreover, lipopolysaccharide-stimulated RAW264.7 cells had higher levels of tumor necrosis factor- $\alpha$ , interleukin-6, and interleukin-1 $\beta$  and showed more CD86-positive cells, whereas the hUC-MSCs co-culture reduced the levels of the three inflammatory cytokines and increased the ratio of CD206-positive cells. The hUC-MSCs treatment inhibited the activation of phosphorylated (p)-C-Jun N-terminal kinase and p-nuclear factor-kappa B not only in liver tissues but also in AML12 and RAW264.7 cells co-cultured with hUC-MSCs. **Conclusions:** hUC-MSCs could alleviate ALF by regulating hepatocyte apoptosis and macrophage polarization, thus hUC-MSC-based cell therapy may be an alternative option for patients with ALF.

**Citation of this article:** Tao Y, Wang Y, Wang M, Tang H, Chen E. Mesenchymal Stem Cells Alleviate Acute Liver Failure through Regulating Hepatocyte Apoptosis and Macrophage

Polarization. J Clin Transl Hepatol 2024;12(6):571–580. doi: 10.14218/JCTH.2023.00557.

## Introduction

Acute liver failure (ALF) is a lethal clinical syndrome with a high mortality rate; it is characterized by severe deterioration in liver function within a short period of time despite no underlying chronic liver diseases.<sup>1</sup> Liver transplantation is the most effective therapeutic option, providing improved outcomes for patients with ALF. However, widespread application of liver transplantation is limited by donor organ shortage and high medical costs.<sup>2</sup> Thus, new therapeutic approaches for ALF are desperately required.

ALF occurs when the rate and extent of hepatocyte death exceed the capacity of liver to repair. The massive death of hepatocytes during ALF progression results in the activation of innate immune cells, leading to the massive production of cytokines and chemokines. The resulting spillover of these inflammatory mediators triggers the development of systemic inflammatory response syndrome (SIRS). Massive liver cell death and disturbed immune and inflammatory responses are distinguishing features that support the development of ALF. It has been speculated that measures inhibiting cell death and the inflammatory storm can prevent the progression of ALF and thus serve as a bridge to liver transplantation. Apoptosis is a model of cell death that finally leads to ALF.<sup>3</sup> Caspases are a central component of the machinery responsible for cell apoptosis. Specific signals in apoptotic cells trigger the initiator caspase (-8, -9, -10), which then activates the executive caspases (-3, -6, -7).<sup>4</sup> The activation of executive caspases is the focal point shared by all apoptotic pathways.

Kupffer cells, tissue-specific macrophages present within the liver, constitute 20–25% of the total non-parenchymal liver cell count and have remarkable significance in innate immunity.<sup>5</sup> Macrophages are highly plastic and adaptable. Traditionally, macrophages are functionally classified into two phenotypes: proinflammatory (M1) and anti-inflammatory macrophages (M2).<sup>6</sup> During the different stages of ALF, hepatic macrophages undergo phenotypic and functional changes to either aggravate injury or promote tissue recovery. The process of macrophage functional transfor-

**Keywords:** Human umbilical cord mesenchymal stem cells; Acute liver failure; Hepatocyte apoptosis; Hepatitis; Macrophage polarization; LPS/D-GalN.

\***Correspondence to:** Hong Tang and Enqiang Chen, Center of Infectious Diseases, West China Hospital of Sichuan University, No.37 Guo Xue Xiang, Wuhou District, Chengdu, Sichuan 610041, China. ORCID: <https://orcid.org/0000-0002-8523-1689> (EC). Tel: +86-28-85422647. Fax: +86-28-85422649. E-mail: htang6198@hotmail.com (HT) and chenengqiang1983@hotmail.com (EC).

mation is known as polarization.<sup>7</sup> During the initiation and propagation phases of ALF, macrophages are triggered and switch to the proinflammatory M1 phenotype because of the injury stimulus, leading to the release of inflammatory cytokines and chemokines that amplify the proinflammatory signal and recruit bone marrow-derived monocytes into the liver to expand the macrophage pool.<sup>8,9</sup> Meanwhile, these macrophage-released inflammatory mediators recruit and activate other circulating immune cells, predominantly dendritic cells, eosinophils, and T cells, thus driving the development of SIRS. During the resolution phase, macrophages undergo functional reprogramming and shift from M1 to M2 phenotype to promote tissue recovery.<sup>10</sup> Therefore, ALF is an immune-driven disorder wherein macrophages are the key determinant of the initiation, propagation, and resolution phases of the disease.<sup>11</sup> Strategies approaching macrophage polarization as the therapeutic target may have the potential to alleviate ALF.

Mesenchymal stem cells (MSCs) are multipotent cells that can self-renew and differentiate into various somatic cells, such as adipose cells, osteocytes, chondrocytes, and hepatocyte-like cells. MSCs also secrete soluble cytokines and participate in immunomodulation.<sup>12</sup> They can be isolated from various human body sites, such as adipose tissue, bone marrow, placental tissue, dermis, and umbilical cord (UC).<sup>13</sup> The UC is a preferred source for MSC isolation given its advantages of abundant resources, ease of collection, and noninvasive collection procedure.<sup>14</sup>

Notably, MSCs have multipotent differentiation potential as well as paracrine and immunomodulatory properties that are exerted via cellular crosstalk and production of bioactive molecules, therefore, MSCs have been widely studied, and their use has been considered a promising strategy for treating various diseases, including liver failure.<sup>15,16</sup> The mechanisms underlying how MSCs can prevent liver failure are complex and remain to be elucidated. In this study, we performed *in vitro* and *in vivo* experiments to explore the role of human UC MSCs (hUC-MSCs) in the treatment of Lipopolysaccharide (LPS)/ D-galactosamine (D-GalN)-induced ALF and the underlying mechanisms, with particular focus on hepatocyte apoptosis and macrophage polarization.

## Methods

### Cell culture and *in vitro* experiments

hUC-MSCs were provided by Hui Rong Tong Chuang Biological Technology Co., Ltd. and were cultured in Dulbecco's modified Eagle's medium (DMEM) containing 20% fetal bovine serum (FBS, Gibco, Grand Island, USA) and 1% penicillin-streptomycin under standard culture conditions (a humidified 5% CO<sub>2</sub> incubator at 37°C). The hUC-MSCs used in the present study were all within passage 5.

AML12, a mouse hepatocyte cell line, was obtained from Haixing Biological Technology Co., Ltd. (Suzhou, China) and cultured in DMEM/F12 containing 1% insulin-transferrin-selenium, 40-ng/mL dexamethasone, and 10% FBS under standard cell culture conditions (5% CO<sub>2</sub>, 95% air). A hUC-MSC/AML12 co-culture system was established to explore the effect of hUC-MSCs on injured hepatocytes *in vitro*. The hUC-MSCs seeded in 6-well plates were cultured overnight. Meanwhile, AML12 cells were cultured in Transwell inserts (0.4- $\mu$ m pores, Falcon) for 12 h. Transwell inserts containing AML12 cells were added to plates preloaded with hUC-MSCs, and then, AML12 cells were stimulated with 150-ng/mL LPS and 50- $\mu$ g/mL D-GalN. The co-culture system was

incubated for 24 h under standard culture conditions. The upper AML12 cells were collected and washed for the following experiments.

The murine macrophage RAW264.7 cell line was incubated in DMEM (HyClone, USA) supplemented with 10% FBS (Gibco, Grand Island, USA) and 1% penicillin-streptomycin at 37°C and 5% CO<sub>2</sub>. A hUC-MSC/RAW264.7 co-culture system was established to explore the effect of hUC-MSCs on macrophage polarization *in vitro*. Briefly, hUC-MSCs seeded in 6-well plates were cultured overnight. The Transwell inserts containing RAW264.7 cells were exposed to LPS (1  $\mu$ g/mL) stimulation and were immediately added to plates preloaded with hUC-MSCs, and the co-culture system was incubated for 12 h under standard culture conditions. The upper RAW264.7 cells were collected for further study.

### Animal experiments

C57BL/6J male mice (6–8 weeks old, weighing 20–25 g) were purchased from Huaxi Laboratory Animal Center of Sichuan University (Chengdu, China). All mice were maintained under controlled conditions (24°C, 55% humidity, and 12-h day/night rhythm) and had ad libitum access to food and water. The mice received human care according to the Institutional Review Board guidelines for compliance with the Animal Protection Act of Sichuan University. The mice were prepared for further study after 1 week of acclimation.

LPS (*Escherichia coli*, 0111:B4) and D-GalN were purchased from Sigma (St. Louis, MO, USA). Mice were randomly divided into the following three groups (n=10/group): the normal control group, LPS/D-GalN group, and LPS/D-GalN + hUC-MSCs group. The mouse model of ALF was induced by simultaneous intraperitoneal injection of LPS (10  $\mu$ g/kg) and D-GalN (700 mg/kg) dissolved in pyrogen-free physiological saline (NS). Mice in the LPS/D-GalN + hUC-MSCs group were injected with approximately  $2.5 \times 10^6$  hUC-MSCs dissolved in 250  $\mu$ L of NS via the tail vein 1 h before LPS/D-GalN administration. To assess the therapeutic effect of hUC-MSCs on ALF, all mice were euthanized by cervical dislocation 7 h after the establishment of the mouse model of ALF induced by LPS/D-GalN, and the liver tissues and serum were collected for further study.

Using the Kaplan-Meier curve, the survival rates of the mice were monitored at different time points for 10 h after LPS/D-GalN administration. The number of alive mice was counted every 2 h after LPS/D-GalN injection.

### Serological assessments of the liver function and cytokines

For liver function assessment, serum alanine aminotransferase (ALT) and aspartate aminotransferase (AST) levels were detected using commercially available enzymatic assay kits (Solarbio® Life Sciences, Beijing, China). To assess the inflammation status in mice, the levels of serum cytokines tumor necrosis factor- $\alpha$  (TNF- $\alpha$ ), interleukin-6 (IL-6), and IL-1 $\beta$  were measured using enzyme-linked immunosorbent assay kits (Neobioscience, Beijing, China) according to the manufacturer's instructions.

### Histological assessment

Hematoxylin-eosin staining (HE) was performed to evaluate histological changes in the liver. Liver tissue was collected, routinely fixed with 4% paraformaldehyde, and then embedded in paraffin. After immobilization, the tissues were cut into 5- $\mu$ m sections. The sections were stained with HE according to a standard protocol and were visualized under a light microscope.

**Table 1. Primer sequences used for real time PCR**

Gene		Primers (5'–3')
TNF- $\alpha$	Forward	ATGGCCTCCCTCTCATCAGT
	Reverse	TTTGCTACGACGTGGGCTAC
IL-6	Forward	TGCAATAACCACCCCTGACC
	Reverse	ATTTGCCGAAGAGCCCTCAG
IL-1 $\beta$	Forward	TGCCACCTTTTGACAGTGATG
	Reverse	ATGTGCTGCTGCGAGATTTG
GAPDH	Forward	CCCTTAAGAGGGATGCTGCC
	Reverse	TACGGCCAAATCCGTTTACA

TNF- $\alpha$ , tumor necrosis factor- $\alpha$ ; IL-6, interleukin-6; IL-1 $\beta$ , interleukin-1 $\beta$ ; GAPDH, Glyceraldehyde 3-phosphate dehydrogenase.

### Immunohistochemistry

The deparaffinized and rehydrated paraffin sections were incubated in the presence of cleaved caspase-3 antibody (Cell Signaling Technology, USA), iNOS antibody (Cell Signaling Technology, USA), and CD206 antibody (Cell Signaling Technology, USA) overnight at 4°C, and then, they were incubated with a biotinylated secondary antibody for 1 h at room temperature (20–25°C). After staining with diaminobenzidine (DAB) and counterstaining with hematoxylin, the sections were observed under a light microscope (40 $\times$ ).

### TUNEL staining

Using the Colorimetric TUNEL Apoptosis Assay Kit (Beyotime Institute of Biotechnology, Jiangsu, China), TUNEL staining was performed to detect apoptotic cells, according to a previous report.<sup>17</sup> Briefly, paraffin sections were routinely deparaffinized, rehydrated, rinsed, and incubated in 20- $\mu$ g/mL protease K. Then, the sections were blocked with 3% H<sub>2</sub>O<sub>2</sub> solution, followed by incubation with the TUNEL reaction mixture. Subsequently, the sections were incubated for 30 min at room temperature with horseradish peroxidase-conjugated streptavidin solution, stained with DAB chromogenic reagent, and dehydrated twice with 95% ethanol for 5 min and then with 100% ethanol. The sections were observed under a microscope.

### Real-time quantitative PCR analysis

Total RNA was extracted from liver tissues using the TRIzol reagent (Invitrogen, USA) according to the manufacturer's instructions. Total RNA was reverse-transcribed using PrimeScript™ RT Master Mix (Takara, Japan). The expression of gene mRNAs was measured by real-time PCR using Maxima SYBR green/ROX qPCR Master Mix (Fermentas Life Sciences, Canada). The primer sequences of GAPDH (the reference) and the target genes TNF- $\alpha$ , IL-6, and IL-1 $\beta$  are listed in Table 1. The relative expression of the target genes was calculated by determining their ratio to GAPDH.

### Flow cytometric assessment

AML12 cell apoptosis was evaluated using an annexin V-fluorescein isothiocyanate apoptosis detection kit (Sigma-Aldrich, USA) following the manufacturer's protocol. Briefly, AML12 cells were collected, washed, and resuspended in 1 $\times$  binding buffer and then stained with the annexin V-fluorescein isothiocyanate conjugate and a propidium iodide solution. After incubation for 15 min in the dark at room temperature, stained cells were analyzed by flow cytometry (Bio-Rad, Hercules, California, USA).

RAW264.7 cells, with or without the co-culture of hUC-MSCs, were collected after LPS stimulation for 12 h and then subjected to fluorescence-activated cell sorting analysis. RAW264.7 cells were centrifuged at 400g for 5 min and resuspended in phosphate-buffered saline and were sequentially incubated at 4°C with anti-mouse CD86 (E-AB-F0994E, Elabscience) and then with anti-CD206 (E-AB-F1135D, Elabscience) for 60 min in the dark, according to the manufacturer's instructions. Then, these RAW264.7 cells were added with flow dye buffer and centrifuged at 400g for 5 min. After removing the supernatant, RAW264.7 cells were resuspended with flow dye buffer and detected by flow cytometry (BD Biosciences, San Diego, CA, USA).

### Western blot analysis

The protein expressions were determined by Western blotting, according to the standard manufacturer's protocol. The antibodies for phosphorylated (p)-NF- $\kappa$ B/NF- $\kappa$ B, p-Jun N-terminal kinases (JNK)/JNK, TNF- $\alpha$ , IL-6, IL-1 $\beta$ , cleaved caspase-3, cleaved caspase-9, iNOS and CD206 were all purchased from Cell Signaling Technology, Inc. (Beverly, MA, USA). The primary antibodies were all diluted 1:800.  $\beta$ -Tubulin and  $\beta$ -actin (Zhong Shan-Golden Bridge Biological Technology CO., Ltd., Beijing, China) were used as internal references. The images of the gels were captured using a Bio-Rad Image Lab (ChemiDoc™ MP Imaging System, Bio-Rad, California, USA). The bands were analyzed using Image J software (National Institutes of Health, MD, USA).

### Statistical analysis

Statistical analysis was performed using SPSS 20.0 software. Independent experiments were repeated three times. Data are presented as mean $\pm$ deviation. The *t* test or the nonparametric Mann-Whitney U test was performed to calculate the differences between quantitative data, as appropriate. The results were considered statistically significant if the *p* value was <0.05.

## Results

### hUC-MSCs decrease serum ALT/AST levels, histological injury, and mortality in mice with LPS/D-GalN-induced ALF

A mouse model of ALF was induced by intraperitoneal injection of LPS/D-GalN. hUC-MSCs were administered through the tail vein 1 h before LPS/D-GalN injection (Fig. 1A). Liver histological examination revealed substantial hepatocyte necrosis and severely damaged liver architecture, along with massive hemorrhage and inflammatory cell infiltration in the LPS/D-GalN group (Fig. 1B). Meanwhile, the levels of ALT and AST were significantly increased in the LPS/D-GalN group compared with the normal control group (Fig. 1C, *p*=0.005). The hUC-MSCs treatment remarkably alleviated the extent of liver injury, which was evidenced by improved liver histology (Fig. 1B) and reduced ALT and AST levels (Fig. 1C, *p*=0.006). Mice in the LPS/D-GalN group began to die at 4 h after LPS/D-GalN administration, and their mortality reached 100% at 9 h. Conversely, mice in the LPS/D-GalN + hUC-MSCs group began to die at 6 h after LPS/D-GalN administration, with 3 out of 10 mice still alive at the end of our observation period (Fig. 1D, *p*=0.028).

### hUC-MSCs inhibit hepatocyte apoptosis during acute liver injury

As shown in Figure 2A, a significant increase was observed in both cleaved caspase-9 and cleaved caspase-3 in the LPS/D-

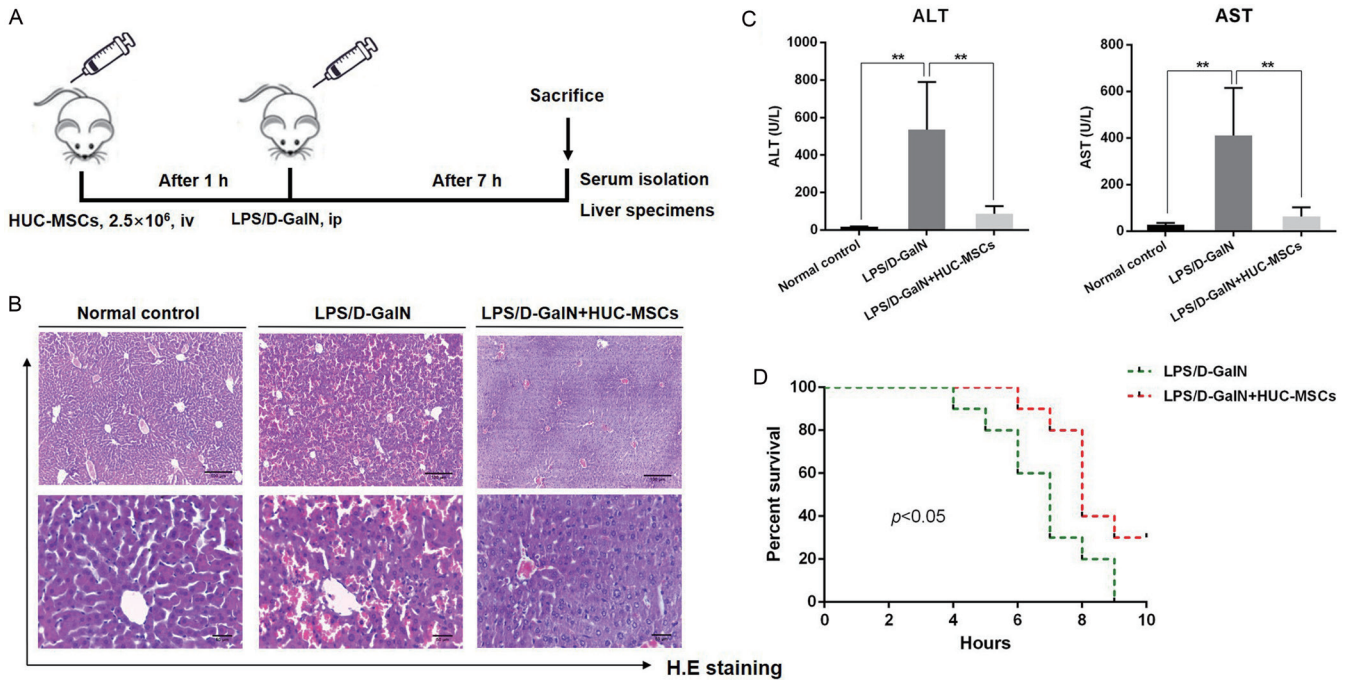


**Fig. 1. The hUC-MSCs treatment alleviated liver injury in LPS/D-GalN-induced ALF.** (A) A schematic of the mouse study. (B) Hematoxylin-eosin staining of liver tissues from the normal control group, LPS/D-GalN group, and LPS/D-GalN+MSCs group. (C) The levels of serum ALT and AST. (D) The survival rates of mice were presented using a Kaplan-Meier curve (n=10/group). \*\**p*<0.01. LPS, lipopolysaccharide; D-GalN, D-galactosamine; ALF, acute liver injury; hUC-MSCs, human umbilical cord mesenchymal stem cells; ALT, alanine amino transferase; AST, aspartate amino transferase.

GalN group, whereas the hUC-MSCs treatment arrested the cleavage of caspase-9 (*p*=0.001) and caspase-3 (*p*=0.021). Correspondingly, TUNEL staining findings revealed significant increases in LPS/D-GalN-induced liver apoptosis, whereas a decrease in apoptotic cells was noted after hUC-MSCs administration (Fig. 1B, *p*=0.005). Meanwhile, IHC results showed more cleaved caspase-3-positive cells in the LPS/D-GalN group (*p*=0.004).

To confirm our above results, the anti-apoptotic effect of hUC-MSCs on LPS/D-GalN-stimulated AML12 cells was further assessed *in vitro*. The flow cytometry findings showed that the hUC-MSC/AML12 co-culture significantly prevented LPS/D-GalN-induced cell apoptosis (21.33±2.038% vs. 33.53±2.027%, *p*=0.013). These data show that hUC-MSCs can alleviate LPS/D-GalN-induced ALF by inhibiting hepatocyte apoptosis.

**hUC-MSCs suppress hepatocyte apoptosis in ALF through inhibiting JNK/NF-κB activation**

We investigated the expressions of some common proteins involved in apoptosis to clarify the mechanisms underlying hUC-MSC-mediated suppression of cell apoptosis, and among these proteins, c-JNK and nuclear factor-kappa B (NF-κB) were widely discussed. As shown in Figure 3A, protein expressions of p-JNK (*p*=0.028) and p-NF-κB (*p*=0.047) were upregulated in the LPS/D-GalN group and downregulated in the LPS/D-GalN +hUC-MSCs group (Fig. 3A).

As shown in Figure 3B, LPS/D-GalN stimulation *in vitro* increased the levels of p-JNK (*p*=0.007) and p-NF-κB (*p*<0.001) in AML cells compared to the normal control group, whereas the hUC-MSCs co-culture downregulated the phosphorylation of both JNK (*p*=0.036) and NF-κB (*p*=0.010). Taken together, hUC-MSCs may suppress hepatocyte apoptosis in LPS/D-GalN-induced ALF by inhibiting JNK/NF-κB activation.

**hUC-MSCs inhibit LPS/D-GalN-induced liver inflammation**

Inflammatory mediators play a vital role in liver failure development, and some common inflammatory factors, such as TNF-α, IL-6, and IL-1β, may be upregulated in ALF.<sup>18,19</sup> Herein, the levels of the proinflammatory factors TNF-α, IL-6, and IL-1β were also measured (Fig. 4). The serum levels of TNF-α (*p*<0.001), IL-6 (*p*<0.001), and IL-1β (*p*=0.009) were found to be significantly increased in the LPS/D-GalN group, and this increase was reversed by the hUC-MSCs treatment (Fig. 4A). Similar differences in the expression of TNF-α, IL-6, and IL-1β genes were also observed at the transcriptional level between the LPS/D-GalN group and the LPS/D-GalN + hUC-MSCs group (Fig. 4B). Protein expression of the three cytokines was dramatically increased in the LPS/D-GalN group compared with the normal control group, and this increase was reversed by hUC-MSCs administration (Fig. 4C).

**hUC-MSCs suppress proinflammatory macrophage M1 polarization and slightly enhance macrophage M2 polarization in the liver**

It is well known that iNOS and CD206 are the biomarkers of M1 and M2 macrophages, respectively.<sup>20</sup> Therefore, we herein measured the levels of iNOS and CD206 to evaluate the macrophage phenotype in liver tissues. The results revealed that iNOS protein levels were increased in the LPS/D-GalN group but decreased in the LPS/D-GalN + hUC-MSCs group (Fig. 4C, *p*=0.009). Conversely, CD206 protein levels were higher in the LPS/D-GalN + hUC-MSCs group than in the LPS/D-GalN group (*p*=0.035). Similarly, the LPS/D-GalN group had more iNOS-positive cells than the normal control group (*p*=0.006) and the LPS/D-GalN + hUC-MSCs group (*p*=0.011), whereas CD206-positive cells were more

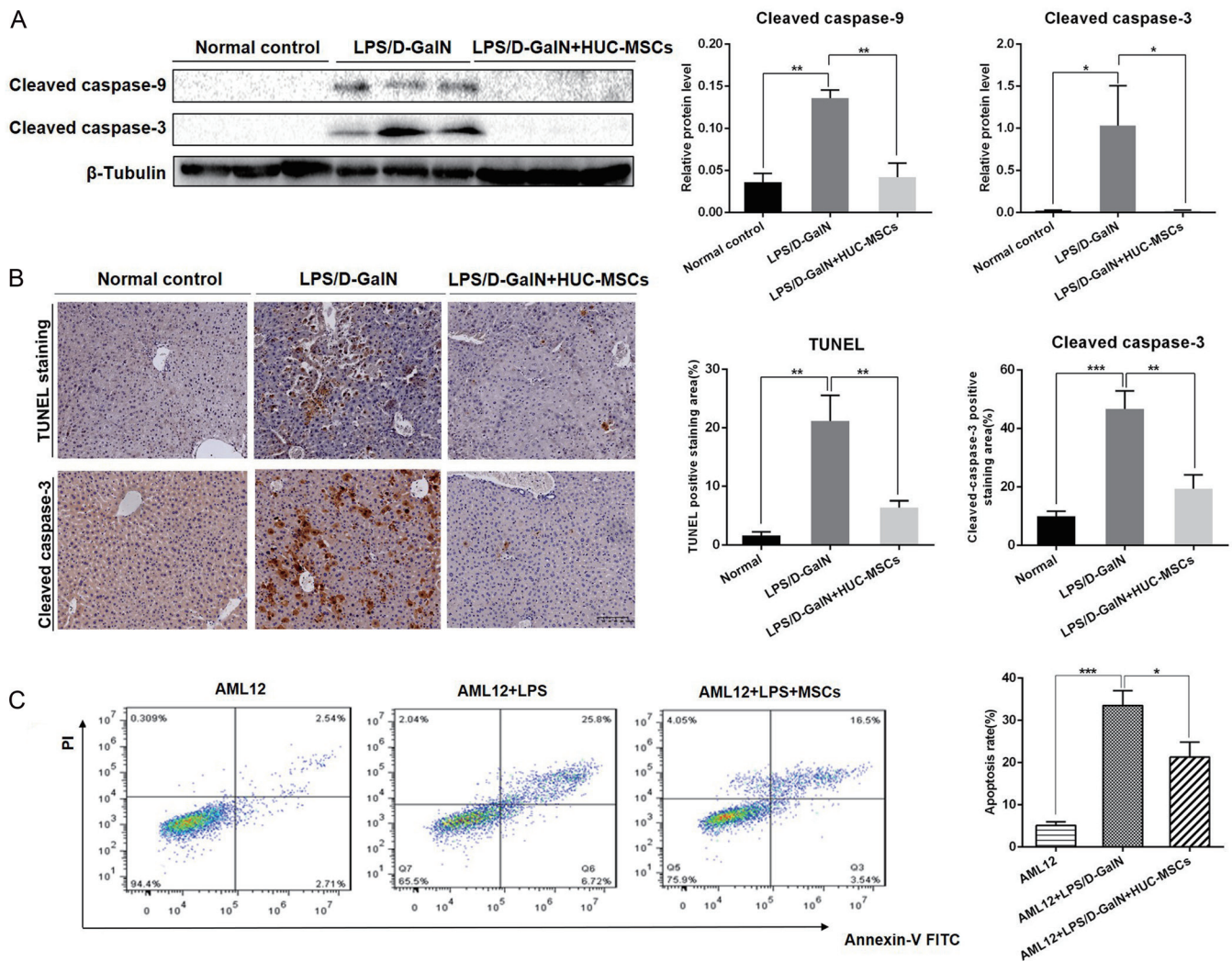


**Fig. 2. hUC-MSCs decreased hepatocyte apoptosis in the liver tissue and AML12 cells.** (A) Protein levels of cleaved caspase 9 and cleaved caspase 3 in the liver tissue were measured and quantified by Western blotting; (B) Hepatocyte apoptosis was detected by TUNEL staining and immunohistochemistry staining, and the results were quantitatively compared. (C) Apoptosis rates in the three groups of normal AML12 cells, AML12 cells treated with LPS/D-GalN, and AML12 cells treated with LPS/D-GalN in the presence of hUC-MSCs were evaluated using flow cytometry. \* $p < 0.05$ , \*\* $p < 0.01$ , \*\*\* $p < 0.001$ . LPS, lipopolysaccharide; D-GalN, D-galactosamine; hUC-MSCs, human umbilical cord mesenchymal stem cells.

abundant in the LPS/D-GalN + hUC-MSCs group (Fig. 4D,  $p = 0.013$ ). These results suggest that hUC-MSCs suppress inflammation in LPS/D-GalN-induced ALF by regulating macrophage polarization.

***hUC-MSCs regulate the phenotype of LPS-stimulated RAW264.7 cells in vitro***

To further demonstrate the role of hUC-MSCs in macrophage phenotype, the RAW.264.7 cell line was used to verify the effect of hUC-MSCs on macrophage polarization. hUC-MSCs were co-cultured with LPS-stimulated RAW264.7 cells. LPS stimulation significantly increased the levels of TNF- $\alpha$ , IL-6, and IL-1 $\beta$  in RAW264.7 cells; however, their co-culture with hUC-MSCs significantly reversed the LPS-enhanced mRNA and protein expression of TNF- $\alpha$ , IL-6, and IL-1 $\beta$  (Fig. 5A, B).

Flow cytometry was used to evaluate the expression levels of the M1 macrophage marker CD86 and the M2 macrophage marker CD206 in RAW264.7 cells (Fig. 6A). LPS stimulation significantly upregulated the expression of CD86,

whereas the hUC-MSCs co-culture decreased the level of CD86 ( $79.33 \pm 3.587$  vs.  $92.28 \pm 1.448$ ,  $p = 0.029$ ). The levels of CD206 were significantly higher in the hUC-MSC-treated group than in the LPS-stimulated group ( $17.06 \pm 2.134$  vs.  $3.473 \pm 0.5660$ ,  $p = 0.004$ ). Furthermore, the protein levels of iNOS and CD206 were also detected using Western blotting. As shown in Figure 6B, the protein expression levels of iNOS were significantly increased in the LPS-stimulated group compared with the hUC-MSC-treated group ( $p < 0.001$ ), whereas the protein expression levels of CD206 were significantly increased in the hUC-MSC-treated group compared with the LPS-stimulated group ( $p < 0.001$ ). These results revealed that hUC-MSCs inhibited LPS-induced M1 polarization and promoted M2 polarization in RAW264.7 cells.

***hUC-MSCs regulate macrophage polarization through the JNK/NF- $\kappa$ B signaling pathway***

To clarify the mechanism underlying the regulation of macrophage polarization by hUC-MSCs, changes in JNK and NF-

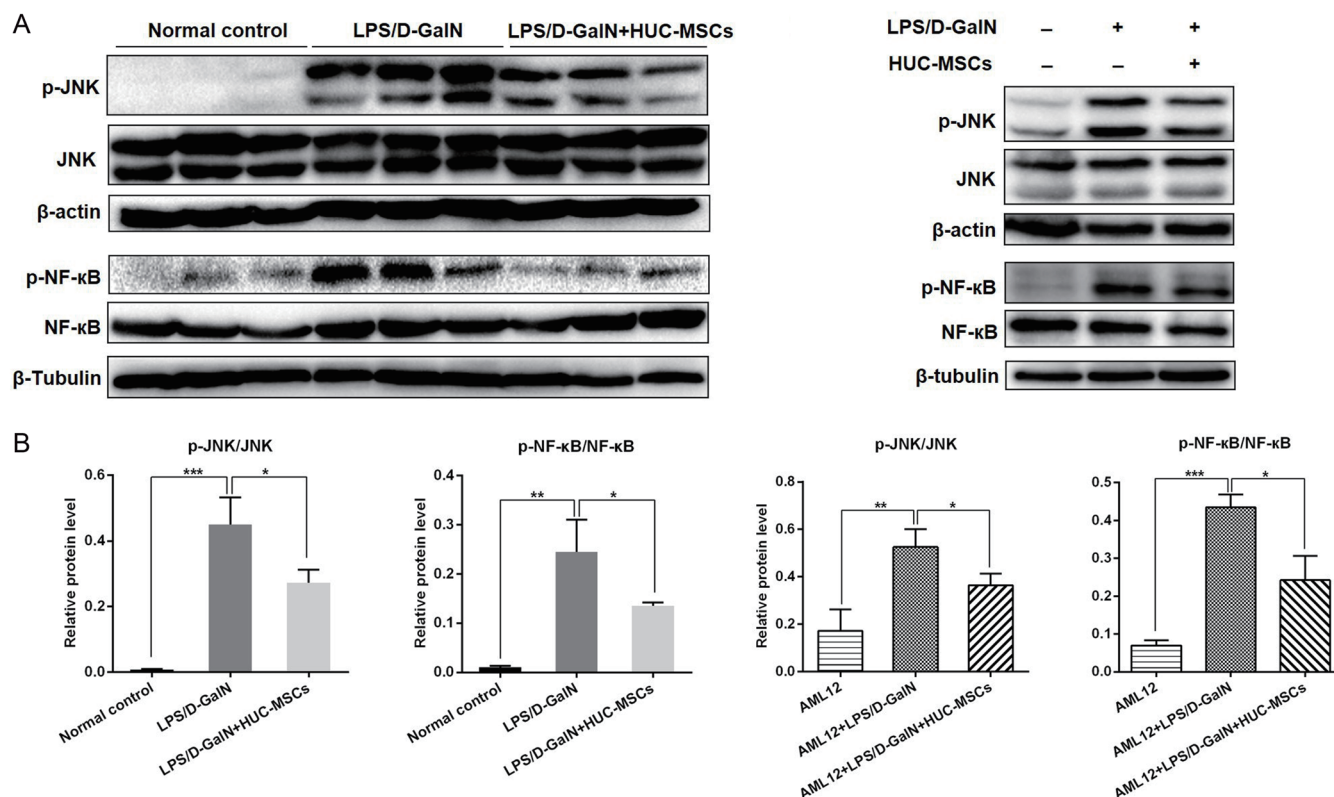


**Fig. 3.** hUC-MSC-adjusted protein levels of p-JNK/JNK and p-NF-κB/NF-κB in the liver tissue (A) and in AML12 cells (B) were measured and quantified by Western blotting. \* $p < 0.05$ , \*\* $p < 0.01$ , \*\*\* $p < 0.001$ . +, with; -, without. hUC-MSCs, human umbilical cord mesenchymal stem cells; JNK, C-Jun N-terminal kinases; NF-κB, nuclear factor-kappa B; LPS, lipopolysaccharide; D-GalN, D-galactosamine.

κB signaling molecules were detected by Western blotting in RAW264.7 cells. As shown in Figure 6, LPS treatment significantly increased the phosphorylation level of JNK ( $p < 0.001$ ) and NF-κB ( $p < 0.001$ ) in LPS-stimulated RAW264.7 cells, whereas hUC-MSCs reduced LPS-induced phosphorylation of JNK ( $p = 0.005$ ) and NF-κB ( $p = 0.015$ ). Taken together, hUC-MSCs can regulate macrophage polarization through the JNK/NF-κB signaling pathway.

## Discussion

In the present study, co-administration of LPS and D-GalN was used to establish the mouse model of ALF as LPS/D-GalN administration has been previously reported to cause typical hepatic apoptosis and systemic inflammation.<sup>21,22</sup> Four hours after LPS/D-GalN administration, liver damage occurred, which was evidenced by damaged liver histology and elevated biochemical indicators. Liver damage in the LPS/D-GalN + hUC-MSCs group was remarkably alleviated by reduced inflammatory cell infiltration and hepatocyte necrosis, decreased ALT and AST levels, prolonged mice survival, and increased number of mice alive at the end of the observation period. Apoptosis is the main pathological feature of LPS/D-GalN-induced ALF. Caspases are closely related to apoptosis induction. Caspase-9 is a major apoptotic initiator and can induce the subsequent cleavage of the apoptotic executioner caspase-3. Activated caspase-3 is responsible for the execution of the final and committed phase of apoptotic cell death.<sup>23</sup> In this study, we observed that the hUC-MSCs treatment significantly suppressed the LPS/D-GalN-stimulated cleavage of caspase-9 and caspase-3 in the liver.

The protective role of hUC-MSCs against LPS exposure was further verified in AML12 cells *in vitro* as hUC-MSC-treated cells showed fewer apoptotic cells than LPS-stimulated cells. These observations showed that hUC-MSCs alleviated LPS/D-GalN-induced ALF by inhibiting hepatocyte apoptosis.

Previous studies have proven that JNK and NF-κB signaling are classical pathways involved in cell apoptosis during acute liver damage.<sup>24–26</sup> In the present study, we observed that hUC-MSCs inhibited LPS-induced JNK and NF-κB phosphorylation in both liver tissues and AML12 cells. Therefore, we speculated that the hUC-MSCs treatment exerts a protective effect against acute hepatic injury by inhibiting hepatocyte apoptosis via the regulation of JNK and NF-κB phosphorylation.

SIRS is among the early main pathogenic events that drive the progression of ALF.<sup>27</sup> Suppressing the excessive inflammatory response may improve the prognosis of ALF. In the present study, LPS/D-GalN administration led to increased levels of some common proinflammatory cytokines, namely TNF-α, IL-1β, and IL-6, the levels of which may be correlated with the poor outcome of ALF mice. The hUC-MSCs treatment significantly decreased the levels of TNF-α, IL-6, and IL-1β, which is consistent with previous findings that substantiate the anti-inflammatory effects of stem cells.<sup>28,29</sup>

Macrophages have a perceptible effect on the progression of SIRS during ALF. They exert different functions in liver inflammation; the proinflammatory M1 phenotype aggravates injury by producing proinflammatory cytokines and chemokines, whereas the anti-inflammatory M2 phenotype promotes tissue repair by producing anti-inflammatory mediators, depending on the signals derived from the tissue

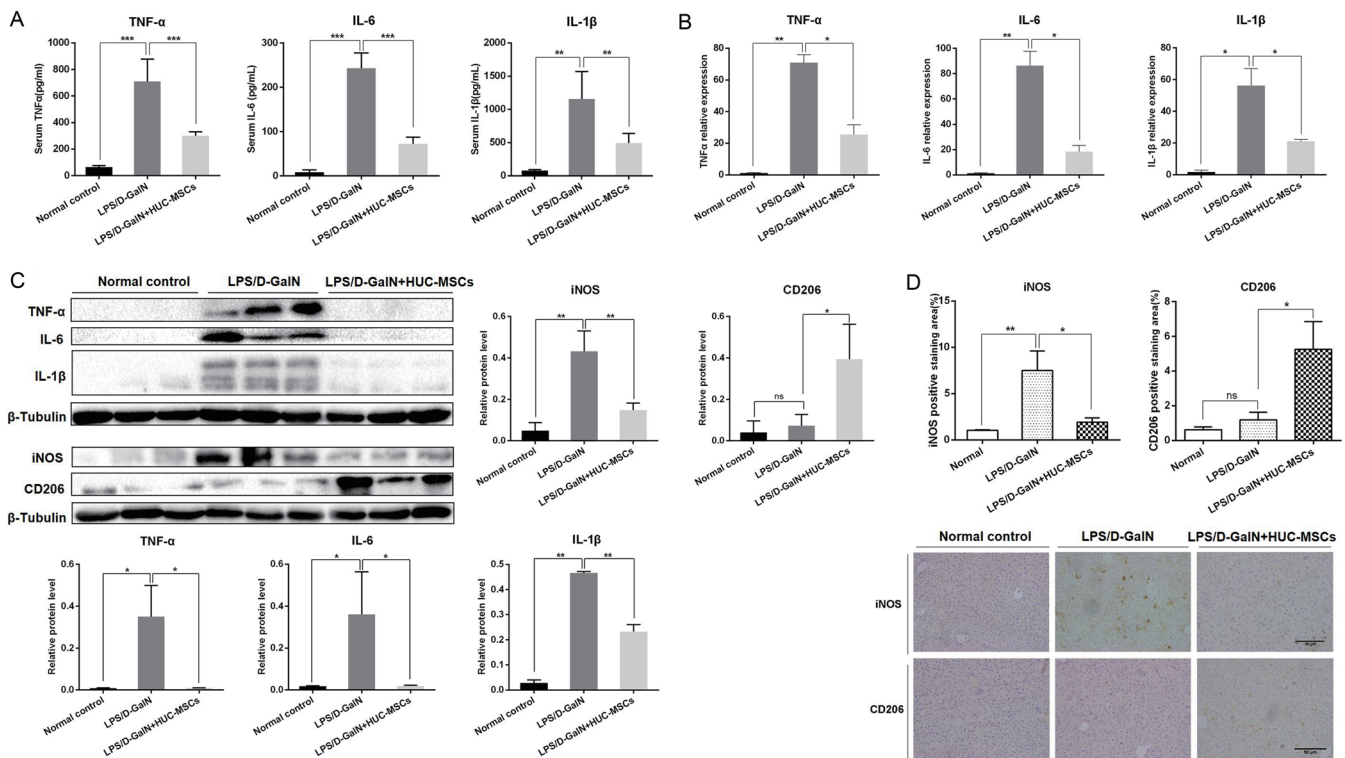


**Fig. 4. The hUC-MSCs co-culture reduced inflammatory cytokine levels and regulated the macrophage phenotype.** (A) ELISA analysis of TNF- $\alpha$ , IL-6, and IL-1 $\beta$  levels in animal serum. (B) Hepatic mRNA levels of the inflammatory cytokines TNF- $\alpha$ , IL-6, and IL-1 $\beta$ . (C) Protein levels of TNF- $\alpha$ , IL-6, IL-1 $\beta$ , iNOS, and CD206 in the liver tissue were measured and quantified by Western blotting. (D) Immunohistochemistry staining analysis of iNOS and CD206 levels in the liver tissue; the results were quantitatively compared. \* $p < 0.05$ , \*\* $p < 0.01$ , \*\*\* $p < 0.001$ . hUC-MSCs, human umbilical cord mesenchymal stem cells; ELISA, enzyme-linked immunosorbent assay; TNF- $\alpha$ , tumor necrosis factor- $\alpha$ ; IL-6, interleukin-6; IL-1 $\beta$ , interleukin-1 $\beta$ ; iNOS, inducible nitric oxide synthase; LPS, lipopolysaccharide; D-GalN, D-galactosamine.

microenvironment.<sup>30,31</sup> Accumulating evidence has proven that MSCs can regulate the balance of M1/M2 macrophage polarization and control the inflammatory response, thus improving the outcome of liver injury.<sup>32,33</sup> LPS is of great significance in initiating immune response and is widely used to explore the role and phenotype of macrophages.<sup>34</sup> In the present study, we observed that the hUC-MSCs treatment inhibited the expression of CD86 and iNOS and promoted the expression of CD206 in both liver tissues and RAW264.7 cells, which is consistent with previous reports stating that MSCs attenuated sepsis-induced liver injury by suppressing macrophage M1 polarization.<sup>33,35</sup> The aforementioned results suggest that hUC-MSCs can protect against LPS/D-GalN-induced ALF through their immunomodulatory properties, as indicated by the regulation of macrophage polarization and the decreased level of circulating inflammatory cytokines.

A better understanding of the exact mechanisms underlying the regulation of macrophage polarization during ALF may be a pivotal step in identifying immune-modulating strategies for liver injury. The JNK and NF- $\kappa$ B signaling pathways have been involved in the regulation of the macrophage phenotype, and their phosphorylation can induce macrophage M1 polarization.<sup>36,37</sup> Regarding molecular mechanisms underlying macrophage polarization, we found both p-JNK and p-NF- $\kappa$ B to be notably increased in LPS-stimulated RAW264.7 cells but decreased after the hUC-MSCs treatment, suggesting that hUC-MSCs suppress LPS-induced macrophage M1 polarization by inhibiting JNK and NF- $\kappa$ B activation.

Numerous studies have proven that MSCs exert protective effects against various insults and challenge ALF in animal models through their anti-inflammatory, anti-apoptotic, anti-

oxidant, and regeneration-stimulating properties.<sup>38-40</sup> In the present study, we proved that hUC-MSCs treatment significantly alleviated LPS/D-GalN-induced ALF primarily through its anti-apoptotic, anti-inflammatory, and immunoregulatory properties; however, the effects of antioxidation and regeneration were not explored. Our observations in the current study had some similarities with the findings of Liu *et al.* who reported that hUC-MSCs could alleviate ALF by inhibiting apoptosis, inflammation, and pyroptosis.<sup>41</sup> Herein, we also investigated the role of macrophage polarization in the treatment of hUC-MSCs for ALF. However, given the limited *in vivo* observation time of hUC-MSCs in our study, we could not determine whether the capacity of hUC-MSCs to differentiate into hepatocyte-like cells played a role in the treatment of ALF.

Besides MSCs, MSC-derived extracellular vesicles, mainly exosomes, have been the focus of research in recent years. MSC-derived exosomes are considered a cell-free approach for ALF with the advantage of stable characteristics, particularly considering that the capacities of MSCs can be impacted by the microenvironment and may be abrogated after some passages.<sup>42,43</sup> Unfortunately, we have neither explored nor discussed the effect of hUC-MSC-derived exosomes on ALF in this study; however, research on the role of exosomes in end-stage liver diseases is currently ongoing.

### Conclusion

In summary, hUC-MSCs can alleviate ALF by inhibiting hepatocyte apoptosis and regulating macrophage polarization, and thus, hUC-MSC-based cell therapy may serve as an alternative option for patients with liver failure.

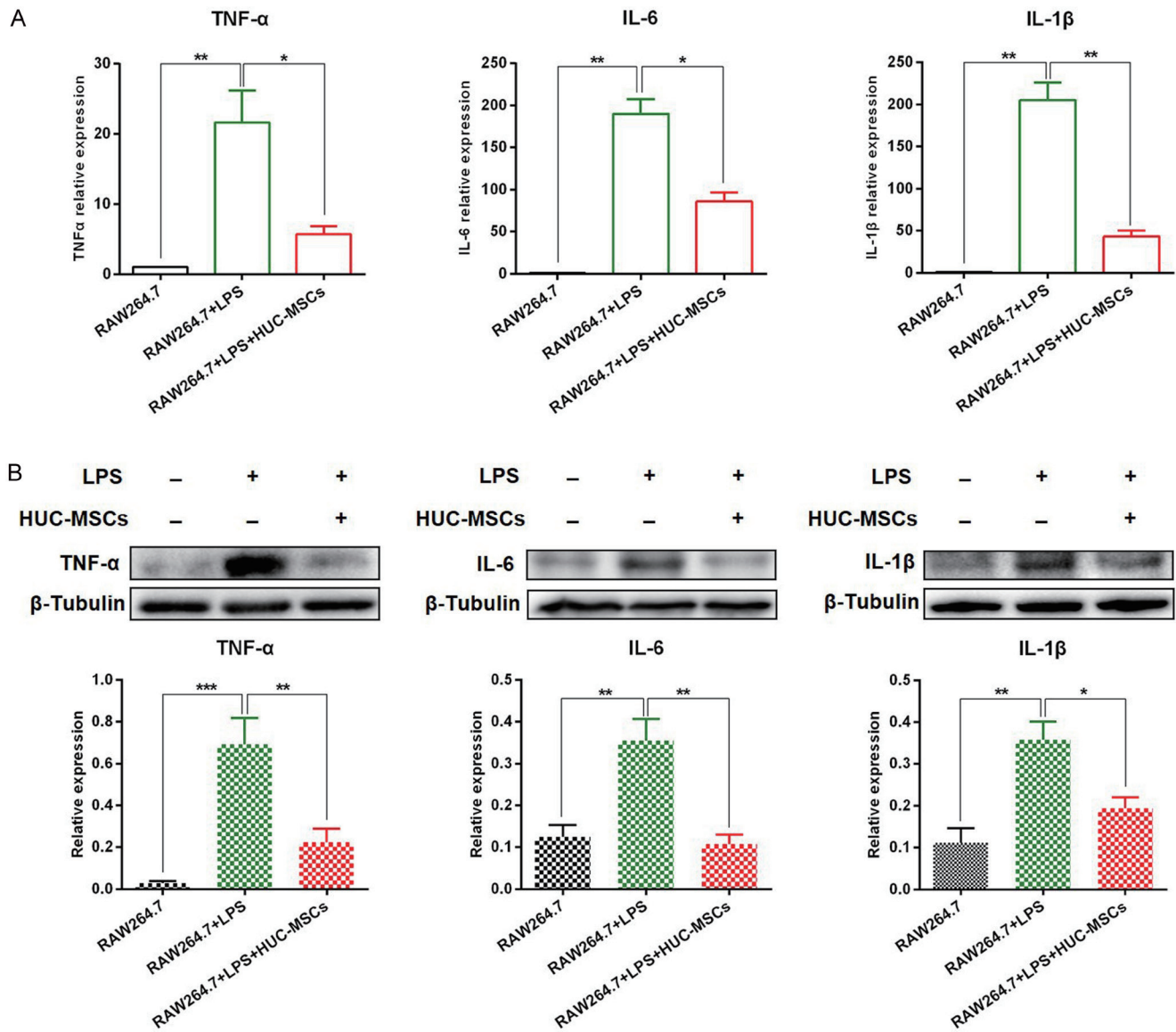


**Fig. 5. The hUC-MSCs co-culture reduced inflammatory cytokine levels in LPS-treated RAW264.7 cells.** (A) Cellular mRNA levels of the inflammatory cytokines TNF- $\alpha$ , IL-6, and IL-1 $\beta$ . (B) Protein levels of TNF- $\alpha$ , IL-6, and IL-1 $\beta$  in the liver tissue were measured and quantified by Western blotting. \* $p$ <0.05, \*\* $p$ <0.01, \*\*\* $p$ <0.001. +, with; -, without; hUC-MSCs, human umbilical cord mesenchymal stem cells; LPS, lipopolysaccharide; TNF- $\alpha$ , tumor necrosis factor- $\alpha$ ; IL-6, interleukin-6; IL-1 $\beta$ , interleukin-1 $\beta$ .

**Acknowledgments**

We thank Medjaden Inc. for scientific editing of this manuscript.

**Funding**

This study was supported by the National Key Research and Development Program of China (2022YFC2304800) and the Science and Technological Supports Project of Sichuan Province in China (2022YFS0094).

**Conflict of interest**

EC has been an Editorial Board Member of *Journal of Clinical and Translational Hepatology* since 2018. The other authors

have no conflict of interests related to this publication.

**Author contributions**

EC and HT proposed the study. YT and YW performed the research. YT, DW, and MW contributed to the acquisition of data and drafting of the manuscript. All the authors contributed to the analysis and interpretation of data and approved the final version of the manuscript.

**Ethical statement**

The animal experiments were approved by the Animal Protection Act of Sichuan University (NO.20220302022). All mice received humane treatment under review of the Institu-



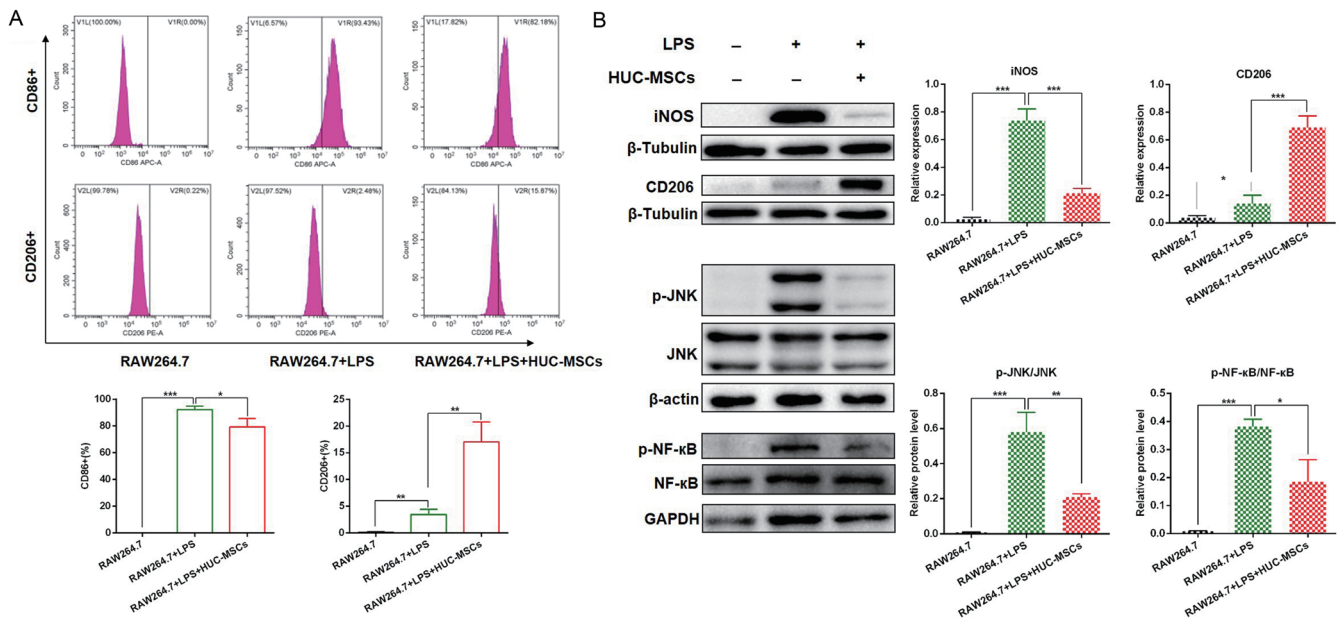


**Fig. 6. The hUC-MSCs co-culture regulated macrophage polarization through the JNK/NF-κB signaling pathway.** (A) The phenotype of RAW264.7 cells was detected by flow cytometry using iNOS and CD206 antibodies. (B) Protein levels of iNOS, CD206, p-JNK/JNK, and p-NF-κB/NF-κB in RAW264.7 cells were measured and quantified by Western blotting. \**p*<0.05, \*\**p*<0.01, \*\*\**p*<0.001. hUC-MSCs, human umbilical cord mesenchymal stem cells; JNK, C-Jun N-terminal kinases; NF-κB, nuclear factor-kappa B; iNOS, inducible nitric oxide synthase; LPS, lipopolysaccharide; GAPDH, Glyceraldehyde 3-phosphate dehydrogenase.

tional Review Board in accordance with the Animal Protection Act of Sichuan University.

**Data sharing statement**

The data used to support the findings of this study are available from the corresponding author upon reasonable request.

**References**

[1] European Association for the Study of the Liver. EASL Clinical Practical Guidelines on the management of acute (fulminant) liver failure. *J Hepatol* 2017;66(5):1047-1081. doi:10.1016/j.jhep.2016.12.003, PMID:28417882.

[2] Dogan S, Gurakar A. Liver Transplantation Update: 2014. *Euroasian J Hepatogastroenterol* 2015;5(2):98-106. doi:10.5005/jp-journals-10018-1144, PMID:29201702.

[3] Rutherford A, Chung RT. Acute liver failure: mechanisms of hepatocyte injury and regeneration. *Semin Liver Dis* 2008;28(2):167-174. doi:10.1055/s-2008-1073116, PMID:18452116.

[4] Bębnowska D, Hryniewicz R, Rzeszotek S, Freus M, Poniewierska-Baran A, Niedźwiedzka-Rystwej P. Apoptotic Cell Death in an Animal Model of Virus-Induced Acute Liver Failure-Observations during Lagovirus europaeus/GI.2 Infection. *Int J Mol Sci* 2024;25(2):798. doi:10.3390/ijms25020798, PMID:38255873.

[5] Xie D, Ouyang S. The role and mechanisms of macrophage polarization and hepatocyte pyroptosis in acute liver failure. *Front Immunol* 2023;14:1279264. doi:10.3389/fimmu.2023.1279264, PMID:37954583.

[6] Murray PJ. Macrophage Polarization. *Annu Rev Physiol* 2017;79:541-566. doi:10.1146/annurev-physiol-022516-034339, PMID:27813830.

[7] Zhang Z, Peng S, Xu T, Liu J, Zhao L, Xu H, *et al*. Retinal Microenvironment-Protected Rhein-GFFYE Nanofibers Attenuate Retinal Ischemia-Repfusion Injury via Inhibiting Oxidative Stress and Regulating Microglial/Macrophage M1/M2 Polarization. *Adv Sci (Weinh)* 2023;10(30):e2302909. doi:10.1002/advs.202302909, PMID:37653617.

[8] Ju C, Tacke F. Hepatic macrophages in homeostasis and liver diseases: from pathogenesis to novel therapeutic strategies. *Cell Mol Immunol* 2016;13(3):316-327. doi:10.1038/cmi.2015.104, PMID:26908374.

[9] Triantafyllou E, Woollard KJ, McPhail MJW, Antoniadis CG, Pissamari LA. The Role of Monocytes and Macrophages in Acute and Acute-on-Chronic Liver Failure. *Front Immunol* 2018;9:2948. doi:10.3389/fimmu.2018.02948, PMID:30619308.

[10] Vannella KM, Wynn TA. Mechanisms of Organ Injury and Repair by Macrophages. *Annu Rev Physiol* 2017;79:593-617. doi:10.1146/annurev-physiol-022516-034356, PMID:27959618.

[11] Pissamari LA, Thurst MR, Wendon JA, Antoniadis CG. Modulation of

monocyte/macrophage function: a therapeutic strategy in the treatment of acute liver failure. *J Hepatol* 2014;61(2):439-445. doi:10.1016/j.jhep.2014.03.031, PMID:24703954.

[12] Hu C, Wu Z, Li L. Pre-treatments enhance the therapeutic effects of mesenchymal stem cells in liver diseases. *J Cell Mol Med* 2020;24(1):40-49. doi:10.1111/jcmm.14788, PMID:31691463.

[13] Fan XL, Zhang Y, Li X, Fu QL. Mechanisms underlying the protective effects of mesenchymal stem cell-based therapy. *Cell Mol Life Sci* 2020;77(14):2771-2794. doi:10.1007/s00018-020-03454-6, PMID:31965214.

[14] Nagamura-Inoue T, Nagamura F. Umbilical cord blood and cord tissue banking as somatic stem cell resources to support medical cell modalities. *Inflamm Regen* 2023;43(1):59. doi:10.1186/s41232-023-00311-4, PMID:38053217.

[15] Wang YH, Chen EQ. Mesenchymal Stem Cell Therapy in Acute Liver Failure. *Gut Liver* 2023;17(5):674-683. doi:10.5009/gnl220417, PMID:36843422.

[16] Wang J, Ding H, Zhou J, Xia S, Shi X, Ren H. Transplantation of Mesenchymal Stem Cells Attenuates Acute Liver Failure in Mice via an Interleukin-4-dependent Switch to the M2 Macrophage Anti-inflammatory Phenotype. *J Clin Transl Hepatol* 2022;10(4):669-679. doi:10.14218/JCTH.2021.00127, PMID:36062289.

[17] Liu L, Wang P, Liang C, He D, Yu Y, Liu X. Distinct effects of Namp1 inhibition on mild and severe models of lipopolysaccharide-induced myocardial impairment. *Int Immunopharmacol* 2013;17(2):342-349. doi:10.1016/j.intimp.2013.06.017, PMID:23831038.

[18] Dong V, Nanchal R, Karvellas CJ. Pathophysiology of Acute Liver Failure. *Nutr Clin Pract* 2020;35(1):24-29. doi:10.1002/ncp.10459, PMID:31840297.

[19] Wang X, Wu L, Zhang Q, Li L, Xie Y, Wan X, *et al*. Methyl 3,4-dihydroxybenzoate protects against d-galN/LPS-induced acute liver injury by inhibiting inflammation and apoptosis in mice. *J Pharm Pharmacol* 2019;71(7):1082-1088. doi:10.1111/jphp.13091, PMID:31032922.

[20] Yang Y, Ni M, Zong R, Yu M, Sun Y, Li J, *et al*. Targeting Notch1-YAP Circuit Reprograms Macrophage Polarization and Alleviates Acute Liver Injury in Mice. *Cell Mol Gastroenterol Hepatol* 2023;15(5):1085-1104. doi:10.1016/j.jcmgh.2023.01.002, PMID:36706917.

[21] Gu L, He X, Zhang Y, Li S, Tang J, Ma R, *et al*. Fluorfenidone protects against acute liver failure in mice by regulating MKK4/JNK pathway. *Biomed Pharmacother* 2023;164:114844. doi:10.1016/j.biopha.2023.114844, PMID:37224750.

[22] Jia F, Deng F, Xu P, Li S, Wang X, Hu P, *et al*. NOD1 Agonist Protects Against Lipopolysaccharide and D-Galactosamine-Induced Fatal Hepatitis Through the Upregulation of A20 Expression in Hepatocytes. *Front Immunol* 2021;12:603192. doi:10.3389/fimmu.2021.603192, PMID:33746949.

[23] Van Oudenbosch N, Lamkanfi M. Caspases in Cell Death, Inflammation, and Disease. *Immunity* 2019;50(6):1352-1364. doi:10.1016/j.immuni.2019.05.020, PMID:31216460.

[24] Wang M, Sun J, Yu T, Wang M, Jin L, Liang S, *et al*. Diacerein protects liver against APAP-induced injury via targeting JNK and inhibiting JNK-mediated oxidative stress and apoptosis. *Biomed Pharmacother* 2022;149:112917. doi:10.1016/j.biopha.2022.112917, PMID:36068777.

[25] Gao LN, Yan K, Cui YL, Fan GW, Wang YF. Protective effect of *Salvia miltior-*

- rhiza and *Carthamus tinctorius* extract against lipopolysaccharide-induced liver injury. *World J Gastroenterol* 2015;21(30):9079–9092. doi:10.3748/wjg.v21.i30.9079, PMID:26290634.
- [26] Zeng B, Su M, Chen Q, Chang Q, Wang W, Li H. Protective effect of a polysaccharide from *Anoectochilus roxburghii* against carbon tetrachloride-induced acute liver injury in mice. *J Ethnopharmacol* 2017;200:124–135. doi:10.1016/j.jep.2017.02.018, PMID:28229921.
- [27] Tujjos S, Stravitz RT, Lee WM. Management of Acute Liver Failure: Update 2022. *Semin Liver Dis* 2022;42(3):362–378. doi:10.1055/s-0042-1755274, PMID:36001996.
- [28] Jiao Z, Ma Y, Liu X, Ge Y, Zhang Q, Liu B, *et al*. Adipose-Derived Stem Cell Transplantation Attenuates Inflammation and Promotes Liver Regeneration after Ischemia-Reperfusion and Hemihepatectomy in Swine. *Stem Cells Int* 2019;2019:2489584. doi:10.1155/2019/2489584, PMID:31827526.
- [29] Yang H, Chen J, Li J. Isolation, culture, and delivery considerations for the use of mesenchymal stem cells in potential therapies for acute liver failure. *Front Immunol* 2023;14:1243220. doi:10.3389/fimmu.2023.1243220, PMID:37744328.
- [30] Tacke F. Targeting hepatic macrophages to treat liver diseases. *J Hepatol* 2017;66(6):1300–1312. doi:10.1016/j.jhep.2017.02.026, PMID:28267621.
- [31] Wang C, Ma C, Gong L, Guo Y, Fu K, Zhang Y, *et al*. Macrophage Polarization and Its Role in Liver Disease. *Front Immunol* 2021;12:803037. doi:10.3389/fimmu.2021.803037, PMID:34970275.
- [32] Li ZH, Chen JF, Zhang J, Lei ZY, Wu LL, Meng SB, *et al*. Mesenchymal Stem Cells Promote Polarization of M2 Macrophages in Mice with Acute-On-Chronic Liver Failure via Mertk/JAK1/STAT6 Signaling. *Stem Cells* 2023;41(12):1171–1184. doi:10.1093/stmcls/sxad069, PMID:37659098.
- [33] Chen Y, Yang L, Li X. Advances in Mesenchymal stem cells regulating macrophage polarization and treatment of sepsis-induced liver injury. *Front Immunol* 2023;14:1238972. doi:10.3389/fimmu.2023.1238972, PMID:37954578.
- [34] Kozłowski HM, Sobocińska J, Jędrzejewski T, Maciejewski B, Działuk A, Wrotek S. Fever-Range Hyperthermia Promotes Macrophage Polarization towards Regulatory Phenotype M2b. *Int J Mol Sci* 2023;24(24):17574. doi:10.3390/ijms242417574, PMID:38139402.
- [35] Liang X, Li T, Zhou Q, Pi S, Li Y, Chen X, *et al*. Mesenchymal stem cells attenuate sepsis-induced liver injury via inhibiting M1 polarization of Kupffer cells. *Mol Cell Biochem* 2019;452(1-2):187–197. doi:10.1007/s11010-018-3424-7, PMID:30178273.
- [36] Lee SM, Son KN, Shah D, Ali M, Balasubramaniam A, Shukla D, *et al*. Histatin-1 Attenuates LPS-Induced Inflammatory Signaling in RAW264.7 Macrophages. *Int J Mol Sci* 2021;22(15):7856. doi:10.3390/ijms22157856, PMID:34360629.
- [37] Zhou L, Zhao H, Zhao H, Meng X, Zhao Z, Xie H, *et al*. GBP5 exacerbates rosacea-like skin inflammation by skewing macrophage polarization towards M1 phenotype through the NF-κB signalling pathway. *J Eur Acad Dermatol Venereol* 2023;37(4):796–809. doi:10.1111/jdv.18725, PMID:36367676.
- [38] Zhang ZH, Zhu W, Ren HZ, Zhao X, Wang S, Ma HC, *et al*. Mesenchymal stem cells increase expression of heme oxygenase-1 leading to anti-inflammatory activity in treatment of acute liver failure. *Stem Cell Res Ther* 2017;8(1):70. doi:10.1186/s13287-017-0524-3, PMID:28320485.
- [39] Huang YJ, Chen P, Lee CY, Yang SY, Lin MT, Lee HS, *et al*. Protection against acetaminophen-induced acute liver failure by omentum adipose tissue derived stem cells through the mediation of Nrf2 and cytochrome P450 expression. *J Biomed Sci* 2016;23:5. doi:10.1186/s12929-016-0231-x, PMID:26787241.
- [40] Zhang Y, Li Y, Li W, Cai J, Yue M, Jiang L, *et al*. Therapeutic Effect of Human Umbilical Cord Mesenchymal Stem Cells at Various Passages on Acute Liver Failure in Rats. *Stem Cells Int* 2018;2018:7159465. doi:10.1155/2018/7159465, PMID:30538751.
- [41] Liu M, He J, Zheng S, Zhang K, Ouyang Y, Zhang Y, *et al*. Human umbilical cord mesenchymal stem cells ameliorate acute liver failure by inhibiting apoptosis, inflammation and pyroptosis. *Ann Transl Med* 2021;9(21):1615. doi:10.21037/atm-21-2885, PMID:34926659.
- [42] Wang J, Ding H, Zhou J, Xia S, Shi X, Ren H. Transplantation of Mesenchymal Stem Cells Attenuates Acute Liver Failure in Mice via an Interleukin-4-dependent Switch to the M2 Macrophage Anti-inflammatory Phenotype. *J Clin Transl Hepatol* 2022;10(4):669–679. doi:10.14218/JCTH.2021.00127, PMID:36062289.
- [43] Shokravi S, Borisov V, Zaman BA, Niazvand F, Hazrati R, Khah MM, *et al*. Mesenchymal stromal cells (MSCs) and their exosome in acute liver failure (ALF): a comprehensive review. *Stem Cell Res Ther* 2022;13(1):192. doi:10.1186/s13287-022-02825-z, PMID:35527304.